NAVY DEPARTMENT

DAVID TAYLOR MODEL BASIN

WASHINGTON, D.C.

EXPERIMENTAL AND THEORETICAL INVESTIGATIONS OF THE MASS-PLUG ACCELEROMETER

by

D.M. Smith

RESTRICTED

March 1946

Report R-267

PERSONNEL

The experimental work was performed by D.M. Smith, assisted by R.G. Hill. R.D. Specht contributed suggestions on the theoretical development. The report was written by Mr. Smith.

EXPERIMENTAL AND THEORETICAL INVESTIGATIONS OF THE MASS-PLUG ACCELEROMETER

ABSTRACT

The performance characteristics of the mass-plug accelerometer are investigated. This accelerometer is designed and constructed for the measurement of shocks on shipboard by the breaking of a plug of known strength. It is shown that the breaking of a plug does not of itself indicate the magnitude of the acceleration which caused the breakage. Frequency relationships are discussed in connection with two types of breakage. For one type, first-cycle breakage, a general analysis is made which applies to any system with a single degree of freedom. Several new experimental techniques are described which may be of use in future shock-damage investigations.

INTRODUCTION

The mass-plug accelerometer is an instrument which was designed to measure peak amplitudes of acceleration. The instrument which has been used on shock tests by field parties from the David Taylor Model Basin (1)* (2) was built after a sample bakelite plug had been obtained from the Materials Testing Laboratory of the New York Navy Yard. This laboratory had been using an accelerometer in which such plugs were incorporated, and had reported favorable results. However, as very little information was available on the performance characteristics of the instrument, tests and a theoretical analysis of the behavior of the instrument were made at the Taylor Model Basin.

The experimental work described in this report was undertaken primarily to determine the consistency of results under duplicable test conditions, but development of a new experimental technique permitted broadening of the scope of the work and made it possible to study the cause of breakage more thoroughly. The tests were divided chronologically into two groups which will be described separately.

DESIGN OF THE MASS-PLUG ACCELEROMETER

The mass-plug accelerometer, a schematic diagram of which is shown in Figure 1, is designed for measuring accelerations in the direction of its vertical axis only. The theory of operation assumes that, when the instrument is subjected to acceleration in the direction of its longitudinal axis, the mass exerts a force on the plug proportional to the acceleration. If this

---

* Numbers in parentheses indicate references on page 20 of this report.

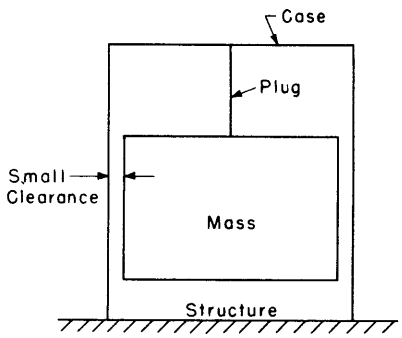

Figure 1 - Schematic Diagram of Mass-Plug Accelerometer

A case attached to the structure has within it a steel mass suspended from a bakelite plug. If the case is pushed upward with sufficient force, the plug will break.

force is of sufficient magnitude, and if the distance through which it travels is sufficient to stretch the neck of the plug to the breaking point, the plug will break at the neck, which will indicate that the value of the acceleration is as great as, or is greater than, the value required for breakage. It is also assumed that all breakage occurs from tension, as when the case receives an upward impulse. Failure through shear or bending is made improbable by constraining the mass to one degree of freedom, and compressional failure is made improbable by the shape of the plug. Since the ratio of the length of the neck to its diameter is small, not exceeding 3 to 1, column buckling cannot take place, and only direct crushing could cause compressional failure. Under the conditions of normal use the large accelerations required to cause crushing do not occur.

The diameter of neck required to obtain failure at a selected value of acceleration may be calculated simply if the possibility of transients is excluded. Let a be the selected value of acceleration. Then

$$F = ma$$

where F is the force applied to the plug and m is the effective mass, i.e., the steel mass plus one-half the plug mass. Also,

$$\sigma_M = \frac{P}{A_1}$$

where σ_M is the ultimate tensile strength of the plug material,

P is the static load in pounds which would cause breakage, and

A_1 is the cross-sectional area of the plug neck in square inches.

Assume that $P = F$, that is, that the dynamic load at failure is equal to the ultimate static load. Then

$$\sigma_M = \frac{F}{A_1}$$

Since $A_1 = \frac{\pi d^2}{4}$, where d is the diameter of the neck in inches,

$$d = \sqrt{\frac{4F}{\pi\sigma_M}} = \sqrt{\frac{4ma}{\pi\sigma_M}} \qquad [1]$$

CONSTRUCTION OF THE ACCELEROMETER

In Figure 2 the parts of the instrument are shown to scale, with the unit mounted on a stud attached to the member that undergoes shock.

The plug itself is made of bakelite. This material was selected because it is easy to machine and has reasonably high tensile strength. The two ends of the plug are threaded, and the midsection or neck is turned down to a predetermined diameter. The length of the neck is kept constant for all diameters.

One end of the plug threads into the mass, which is made of steel and weighs 0.135 pound; the other end threads into the cap. This assembly fits into the case so that the mass has a few thousandths of an inch side clearance and sufficient bottom clearance to permit breakage of the plug. All threads are cut for a tight hand fit and normally the plugs tighten before the last one or two turns are made. Plugs that fail to tighten in this way are discarded.

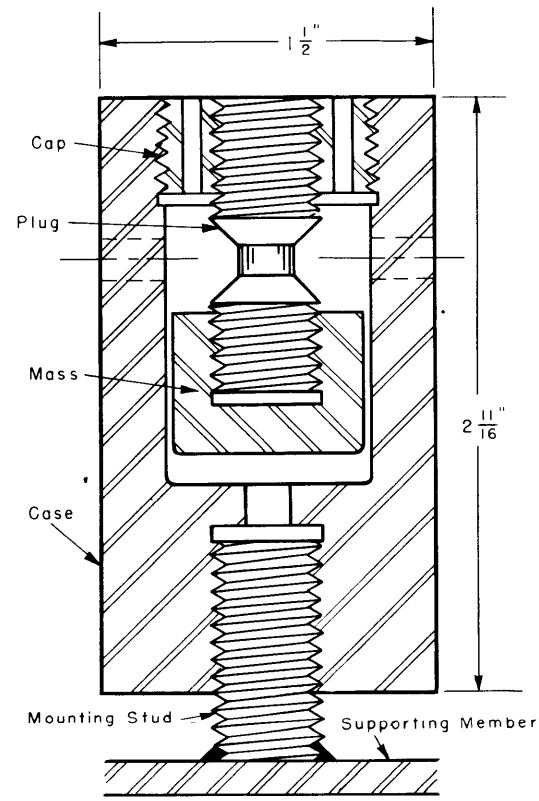

Figure 2 - Mass-Plug Accelerometer

SUITABILITY FOR FIELD TESTS

This instrument has many desirable features as well as some deficiencies. Some desirable features are: simplicity of construction, freedom from mechanical or electrical failures, portability and small size, unidirectional response, and ease of operation. Some deficiencies are that the instrument does not give a time-record of the acceleration; reasonable estimates of the accelerations expected on tests are required beforehand, as well as a sufficient number of sizes of plugs to bracket closely these estimated

values; the method of calculation is based on the assumption that breakage is due to the magnitude of the acceleration only; and frequency, velocity, and displacement are neglected.

TEST METHODS, FIRST GROUP

In the first tests, a wooden destroyer-escort model 20 feet long served as the shock table, as shown in Figure 3. It was floated in the water of the high-speed basin. Underwater charges of tetryl weighing 0.75 ounce each were used to produce the explosive shocks. The charges were placed at a depth of 40 inches below the water surface, but at varying horizontal distances astern of the model. The plugs used were designed to break at an acceleration of 200 g, that is, 200 times gravity. Plugs of this size are about the smallest that it is practicable to make. Whereas greater accuracy could probably have been obtained if larger sizes had been used, they would have necessitated increasing the charge or decreasing its distance from the ship model. This, in turn, would have greatly increased the probability of damaging the model itself.

Some mass-plug units were mounted on a steel plate attached to the inside of the model, and others directly on the wood. The steel plate was used because it seemed a more secure way of mounting the units to the model. Since it was not known definitely that it would be, however, studs were also inserted into the wood for experimental comparison. After the charges had been fired, the units were removed and examined for breakage. Further data

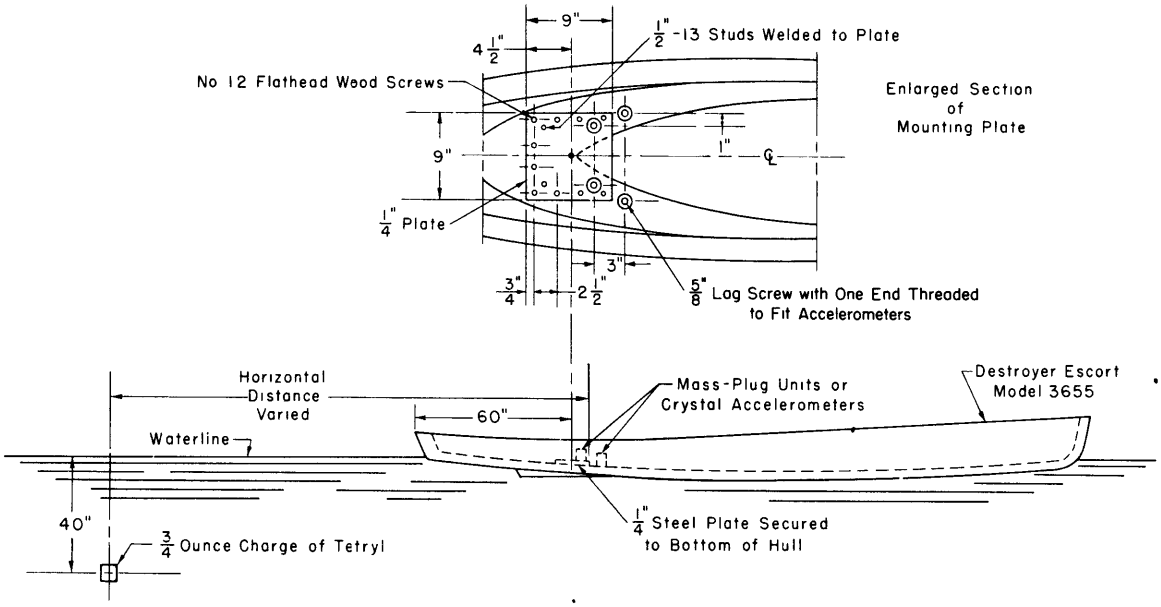

Figure 3 - Experimental Arrangement for Dynamic Tests

were obtained by substituting crystal accelerometers for the mass-plug units, and using cathode-ray oscillograph channels with recording cameras to make records of the acceleration-time curve of both the steel mounting plate and the wood.

TEST RESULTS, FIRST GROUP

The results of the first series of tests are presented in Table 1. Although the wood-mounted plug units were located at a slightly greater distance from the charges than were the steel-mounted units, at some charge positions the wood-mounted plug units ruptured although those mounted on the plate did not. Viewing the results from the two mountings separately, it may be seen that the plugs were reasonably consistent in their behavior. At large horizontal distances all the plugs withstood the attack; at small distances all failed. There is an intermediate range of about 12 inches where some plugs failed and others did not. It may also be seen from Table 1 that the crystal-accelerometer records taken with the charges at the critical distances,* allowing for the 12-inch variation noted, gave an acceleration on the wood between 350 g and 370 g and on the metal between 200 g and 230 g.

TABLE 1

Number of Plugs Broken at Varying Charge Distances and Corresponding Peak Accelerations

Some of the values for peak acceleration were obtained by interpolation of observed values at distances slightly different from those listed. The values at the critical distances, however, are observed values.

Horizontal Distance inches	Plugs Mounted on					
	Wood			Metal		
	Number of Plugs Used	Number of Plugs Broken	Peak Acceleration g	Number of Plugs Used	Number of Plugs Broken	Peak Acceleration g
114	2	0	350	2	0	47
108	2*	1	363	2	0	51
102	2	2	370	2	0	63
96	2	2	392	2	0	80
90	4	4	434	4	0	140
84	4	4	480	4	0	200
78	4	4	523	4*	3	212
72	5	5	560	6	6	230

* These plugs were located at the critical distance.

* The term critical distance will be used to denote the maximum horizontal distance from the boat at which the charge could be placed and still cause failure of the plugs.

DISCUSSION OF RESULTS, FIRST GROUP

The results of the first series of tests were surprising in that the method of mounting affected the value of acceleration required to cause failure and in that, especially for the wood-mounted units, the acceleration causing failure greatly exceeded the value of 200 g predicted from elementary theory. The crystal-accelerometer records revealed that there was also a difference in frequency of vibration of the two mountings. The initial cycle on the wood had a shorter period than that on the metal plate. Since the metal plate introduced an additional mass, and to some extent a spring, between the hull and the plug, this difference was not entirely unexpected, but it seemed desirable to investigate further its possible relation to mass-plug rupture. The most logical way of doing this was to devise a method for finding the time it took the plugs to break after the acceleration had started.

TEST METHODS, SECOND GROUP

The first step in the later series of tests was to silver-plate the bakelite plugs by the Brashear process. This process consists in precipitating metallic silver out of an ammoniacal silver nitrate solution, and allowing it to deposit on the object to be silvered. The advantage of this plating was that the plugs were made into excellent electrical conductors without otherwise altering appreciably their physical characteristics.

After a plug had been silvered, a wire was connected to each of the threaded ends and the two wires were run up through the cap where they were connected into a coupling circuit as shown in Figure 4.

It may be seen from this diagram that, when a plug is broken, there is generated across R_1 an instantaneous voltage which falls off as the capacitor C charges. This voltage is sufficient to give a visible deflection on a cathode-ray oscillograph. To a certain extent the silver plating also acts

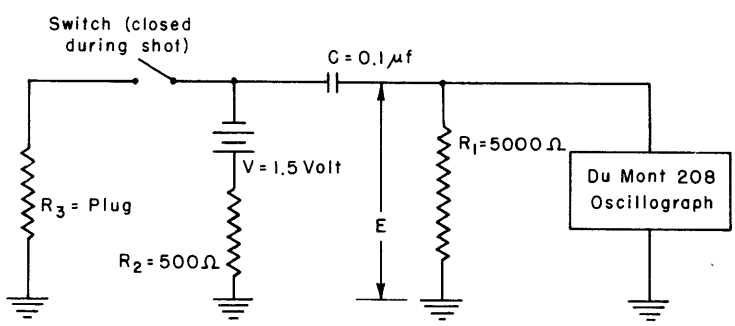

Figure 4 - Circuit Used with Coated-Plug Accelerometers

as a strain gage, since any variation in the resistance of the plating caused by strain in the plug will show up as a voltage change across R_1.

Two oscillograph channels were used to make simultaneous recordings of crystal-accelerometer data and mass-plug-breakage data. This permitted comparison of time to failure with the time of initiation of the acceleration.

DETERMINATION OF NATURAL FREQUENCY

It appeared at this point that, before a completely comprehensive analysis could be made of the significance of the time to failure in relation to the time of the initiation of the acceleration, it would be necessary to determine the natural frequency of the plugs. Since an accurate theoretical calculation of this frequency was difficult because of the geometrical configuration, experimental methods were used.

The first method involved mounting the plug and its associated mass on a rigid support and vibrating the system with an electromagnet which was connected to a variable-frequency electrical oscillator. The magnet was placed under the mass so that only a small clearance existed, and the oscillator frequency was varied until the sound of the mass and magnet striking against each other became audible. Only one frequency gave this condition, but this frequency seemed so low that, as a check, the modulus of bakelite was computed from this value, from the mass, and from the dimensions of the plug neck which was considered to act as a spring. The computation follows:

Given f, the observed frequency in cycles per second, and m, the known mass in pound-seconds^2 per inch, then

$$\omega_0 = \sqrt{\frac{K}{m}}$$

and

$$K = \omega_0{}^2 m = (2\pi f)^2 m$$

where ω_0 is the natural circular frequency and K is the spring constant in pounds per inch. The expression for the elastic modulus is

$$E = \frac{Kl}{A_1} = \frac{4Kl}{\pi d^2}$$

where d is the diameter of the plug neck in inches and l is the length of the plug neck in inches.

The value of the elastic modulus obtained in this manner is subject to some error because of the assumption that all strain takes place in the neck. However, its comparison with handbook values for Young's modulus of

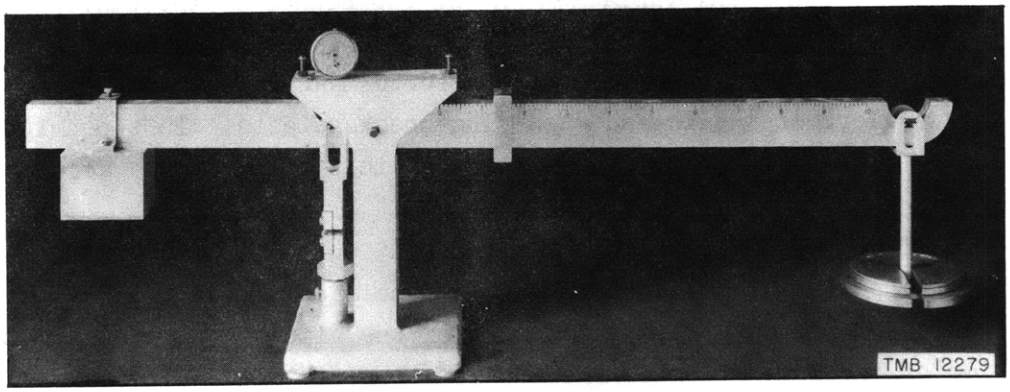

Figure 5a - General View

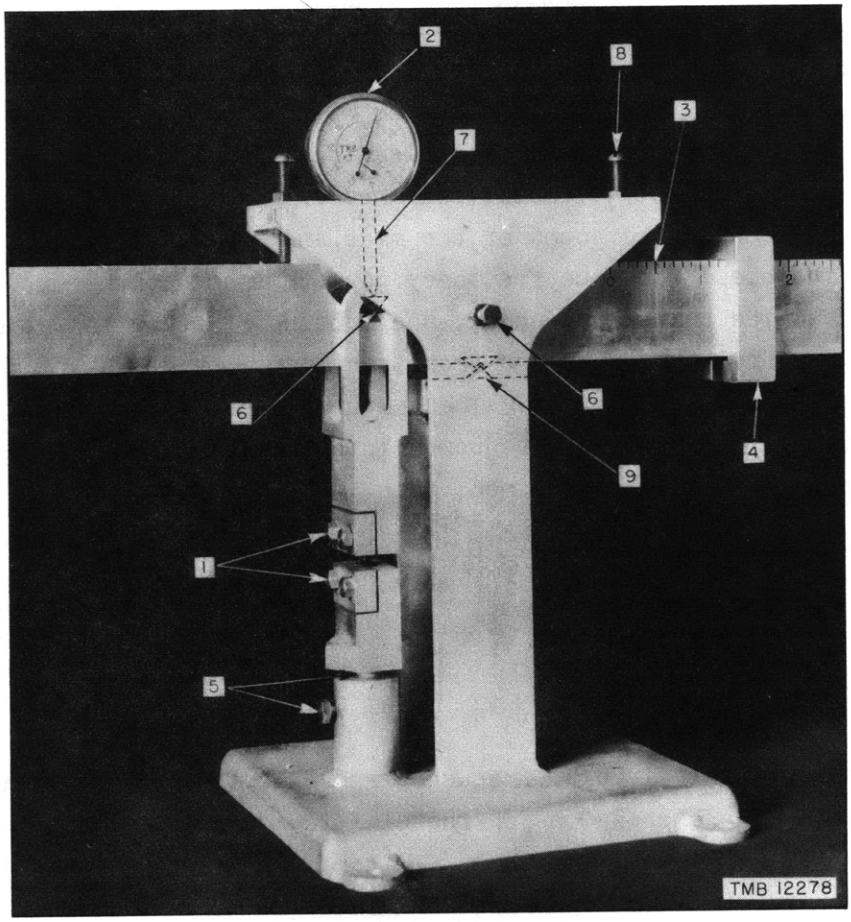

Figure 5b - Close-Up

1. Clamps for specimen
2. Dial gage for reading elongation
3. Scale graduated in pounds for measuring load on specimen
4. Sliding weight for applying load
5. Screw for adjusting length of specimen
6. Centering bolt
7. Pointer of dial gage
8. Clamping bolts to protect knife edges when instrument is not being used
9. Knife-edge pivot on arm

Figure 5 - Tensile-Testing Machine Used for Determining Mass-Plug Spring Constant

bakelite showed so large a discrepancy that the observed frequency value itself was considered questionable. On closer check it developed that the observed frequency was the natural frequency of the magnet and that there was not sufficient power to excite the plug at the higher frequency required for the plug to resonate. If a suitable magnet and oscillator had been available, however, this method would have been the fastest and most accurate way of making the necessary frequency determinations.

The method finally used required the design and construction of a small tensile-testing machine, shown in Figure 5. By use of this device, load-elongation curves for the plugs themselves were obtained. From these curves the spring constant K was found, and by substituting its value in the relation $\omega_0 = \sqrt{K/m}$ the circular frequency ω_0 was calculated. Dividing ω_0 by 2π gave the natural frequency, which for the 200-g plugs was about 720 cycles per second.*

TEST RESULTS, SECOND GROUP

The records obtained from the breakage-time tests on the plated plugs were of two distinct types; namely, those where failure occurred within a fraction of a millisecond after the start of the acceleration, and those where breakage occurred after a much longer interval of time or not at all. Figure 6 is an example of the first type, which was the most common. A summary of the data for this type is given in Table 2. Figures 7, 8, and 9 are

TABLE 2

Time Delay to Breakage

The charge was 3/4 ounce of tetryl.

Mass-Plug Accelerometer Mounted on Wood		Mass-Plug Accelerometer Mounted on Metal	
Horizontal Distance inches	Average Time* Delay milliseconds	Horizontal Distance inches	Time* Delay milliseconds
72	0.15	72**	0.47
78	0.17	72**	0.50
84	0.23	72**	0.55
96	0.19	72**	0.78
108**	0.28	Average delay for 72 inches is 0.56 milliseconds	

* Probable error in measuring records is about 8 per cent.

** These are critical distances.

* The modulus of the bakelite was measured in tension only; the computations apply to tension cycles only.

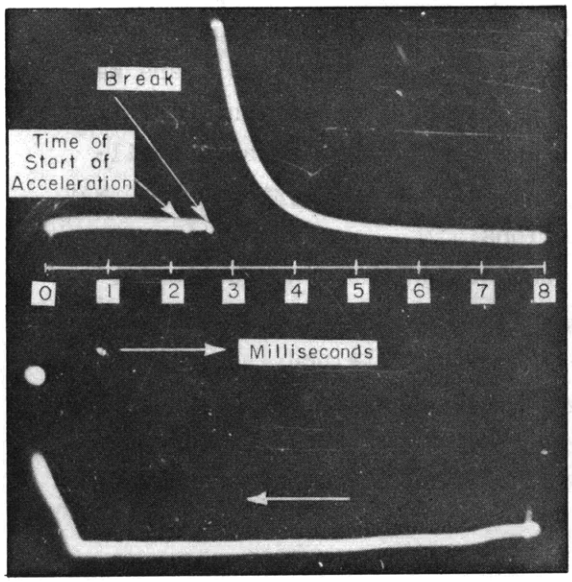

Figure 6 - Breakage Record Most Frequently Observed

There is no amplitude scale. The point at which the acceleration started is indicated. Zero time corresponds to the time of detonation of the charge.

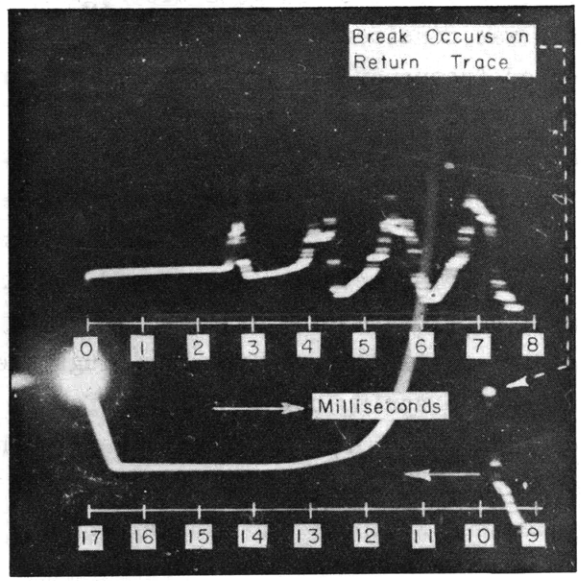

Figure 7 - Record Showing Resonance Build-Up and Failure

This record indicates increasing strain for 4 cycles and breakage on the fifth. There are no displacement-scale values. The observed frequency is 620 cycles per second.

The small time constant of the recording circuit shown in Figure 4 probably accounts for a large part of the distortion evident in the wave form.

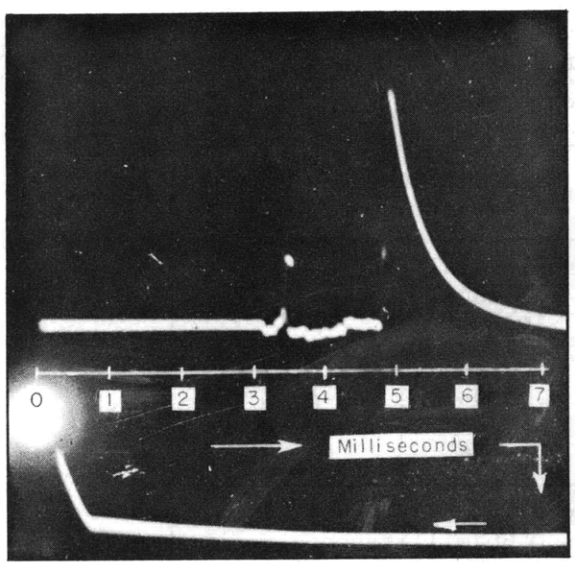

Figure 8 - Record Showing Breakage During Second Cycle

From the first two cycles, the observed frequency appears to be 750 cycles per second.

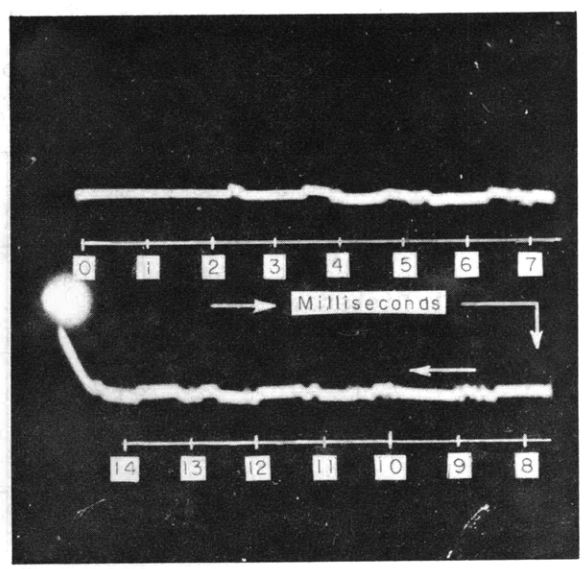

Figure 9 - Record Showing Successive Stress Cycles without Breakage

The observed frequency is 710 cycles per second.

examples of the second type, for which it was not possible to tabulate the data.

Two crystal-accelerometer records which were taken simultaneously with two of the breakage records are shown in Figures 10 and 11, but it should

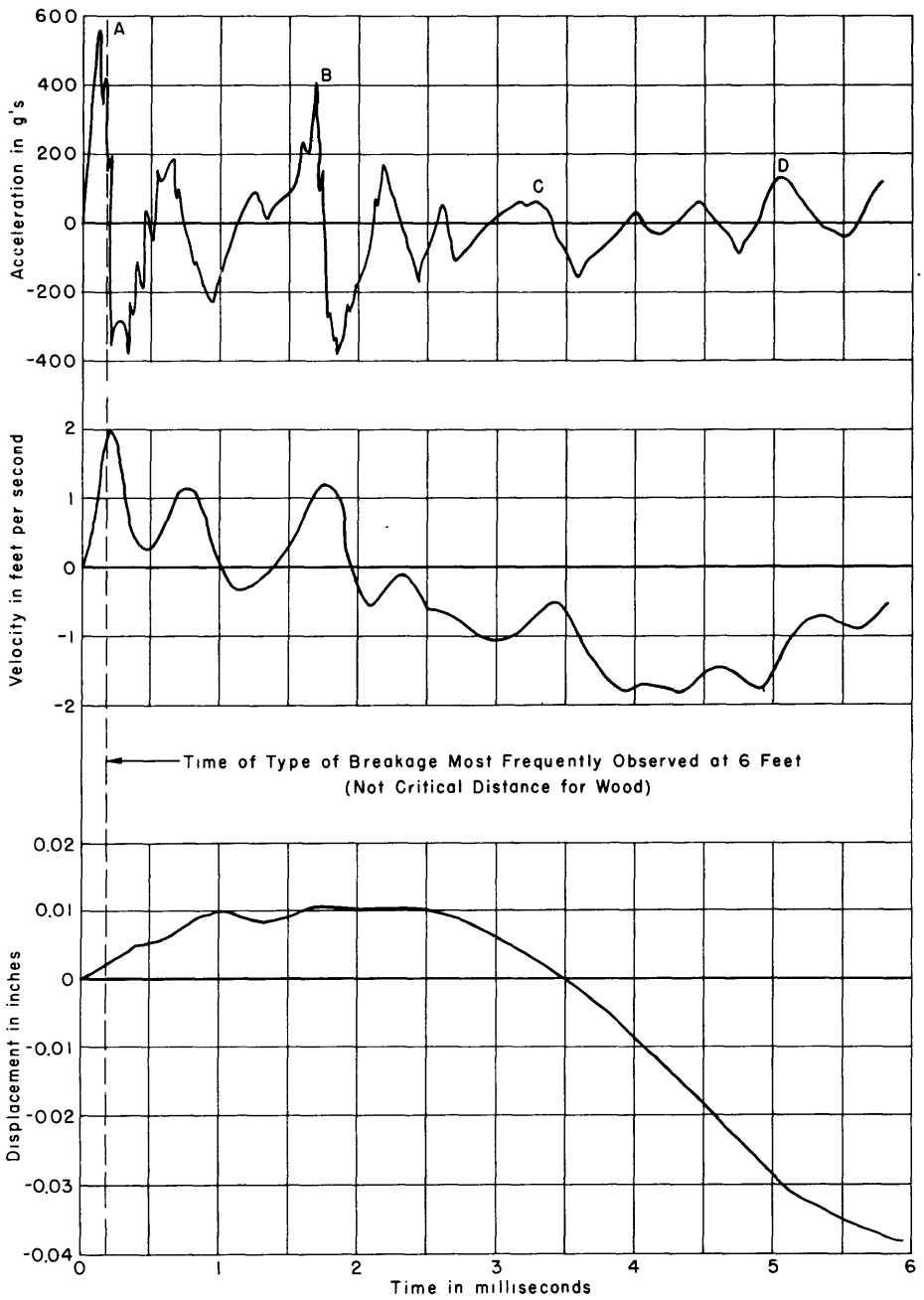

Figure 10 - Records Obtained with Accelerometer Mounted on Wood

The charge, 3/4 ounce of tetryl, was detonated at a distance of 6 feet. Peaks A, B, C, and D indicate components of frequency which produced resonance in Figure 7.

be noted that the record with the accelerometer mounted directly on the wood is taken at 6 feet and not at the critical distance of 8 feet 6 inches. The records for each type of mounting, for all distances and shots, however, showed the same frequency pattern and differed only in the magnitudes of their corresponding peaks.

DISCUSSION OF RESULTS, SECOND GROUP

Since the results of the breakage-time tests showed that breakage did not coincide with peak acceleration but occurred at a later time, it became obvious that an analysis could not be made when only the peak accelerations and static breaking strengths of the plugs were considered. It was for this reason that the acceleration curves of Figures 10 and 11 were integrated, once to give velocity, and again to give displacement. Then the average breakage times for both wood and metal from Table 2 were superimposed on the curves of Figures 10 and 11 as shown by the dotted lines. Even a study of these relations, however, did not explain the time delay or the delay

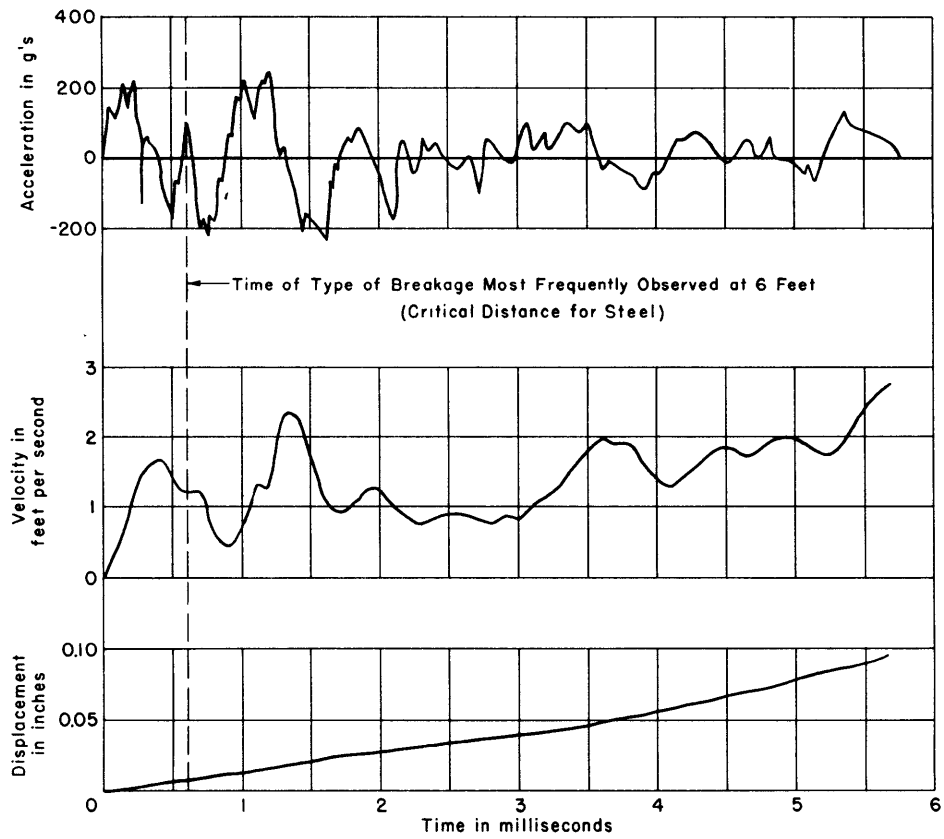

Figure 11 - Records Obtained with Accelerometer Mounted on Metal Plate

The charge, 3/4 ounce of tetryl, was detonated at a distance of 6 feet.

difference between wood and metal. It was apparent that detailed dynamic analysis was necessary.

For clarity the detailed analysis is broken into two separate parts. The first takes up the type of breakage shown in Figure 6 and Table 2 and will be called first-cycle breakage. The second is the type shown in Figures 7 and 8 and will be designated as delayed breakage due to resonance.

FIRST-CYCLE BREAKAGE

In the crystal-accelerometer records the initial acceleration cycle roughly approximates a sine curve when the instrument is mounted on either metal or wood. This permits the assumption of sinusoidal relationships in evolving a theory to account for the time difference between breakage on wood and on metal. It also seems justified to assume that the damping in the mass-plug system is negligible, since it would be small under any conditions, and where only the first cycle is considered its effect is still less.

The equivalent mass-spring system of the mass-plug accelerometer is shown in Figure 12. The force equation for this system (3) (4) is

$$m \frac{d^2y_2}{dt^2} + K(y_2 - y_1) = 0 \qquad [2]$$

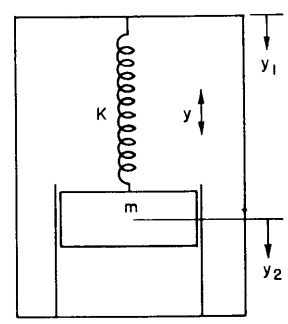

Figure 12 - Equivalent Mass-Spring System

where m is the mass,

K is the spring constant,

y_1 is the absolute displacement of the case, and

y_2 is the absolute displacement of the mass.

Let y be the relative displacement of mass to case; then

$$y = y_2 - y_1 \qquad \text{and} \qquad y_2 = y + y_1$$

When y_2 is eliminated by substituting its equivalent, an equation results which involves only the quantities of interest, that is, the relative displacement y, and the absolute displacement y_1 of the case:

$$m \frac{d^2(y + y_1)}{dt^2} + Ky = 0 \qquad [3]$$

Dividing through by m and transposing yields

$$\frac{d^2y}{dt^2} + \frac{Ky}{m} = -\frac{d^2y_1}{dt^2}$$

or

$$\frac{d^2y}{dt^2} + \omega_0{}^2 y = -\frac{d^2y_1}{dt^2} \qquad [4]$$

where $\omega_0 = \sqrt{K/m}$ is the natural circular frequency of the mass on the spring.

Since it is assumed that the initial cycle of the applied acceleration is sinusoidal,

$$-\frac{d^2y_1}{dt^2} = a_0 \sin \omega t \qquad [5]$$

where a_0 is the positive peak acceleration on the first cycle and can be taken from an acceleration record obtained at the critical distance, and ω is the circular frequency of this first cycle. Then

$$\frac{d^2y}{dt^2} + \omega_0{}^2 y = a_0 \sin \omega t \qquad [6]$$

The solution of Equation [6] is

$$y = A \sin \omega_0 t + B \cos \omega_0 t + \frac{a_0}{\omega_0{}^2 - \omega^2} \sin \omega t \qquad [7]$$

The equations for velocity and acceleration can be obtained by successive differentiations of Equation [7], and since experimental records show that the boundary conditions are $y = 0$, $dy/dt = 0$, at $t = 0$, the constants A and B may be evaluated with the following results:

$$A = -\frac{\omega}{\omega_0} \frac{a_0}{\omega_0{}^2 - \omega^2}$$

$$B = 0$$

Therefore

$$y = \frac{a_0}{\omega_0{}^2 - \omega^2} \sin \omega t - \frac{\omega}{\omega_0} \frac{a_0}{\omega_0{}^2 - \omega^2} \sin \omega_0 t \qquad [8]$$

Numerical values of a_0 and ω can be estimated from crystal-accelerometer data; the value of ω_0 has been given above. Therefore the elongation y of the stem of the accelerometer is completely determined as a function of time.

Computed curves of y against t for both wood and steel mountings at the respective critical distances are shown in Figure 13, where t is plotted in milliseconds and y in inches.

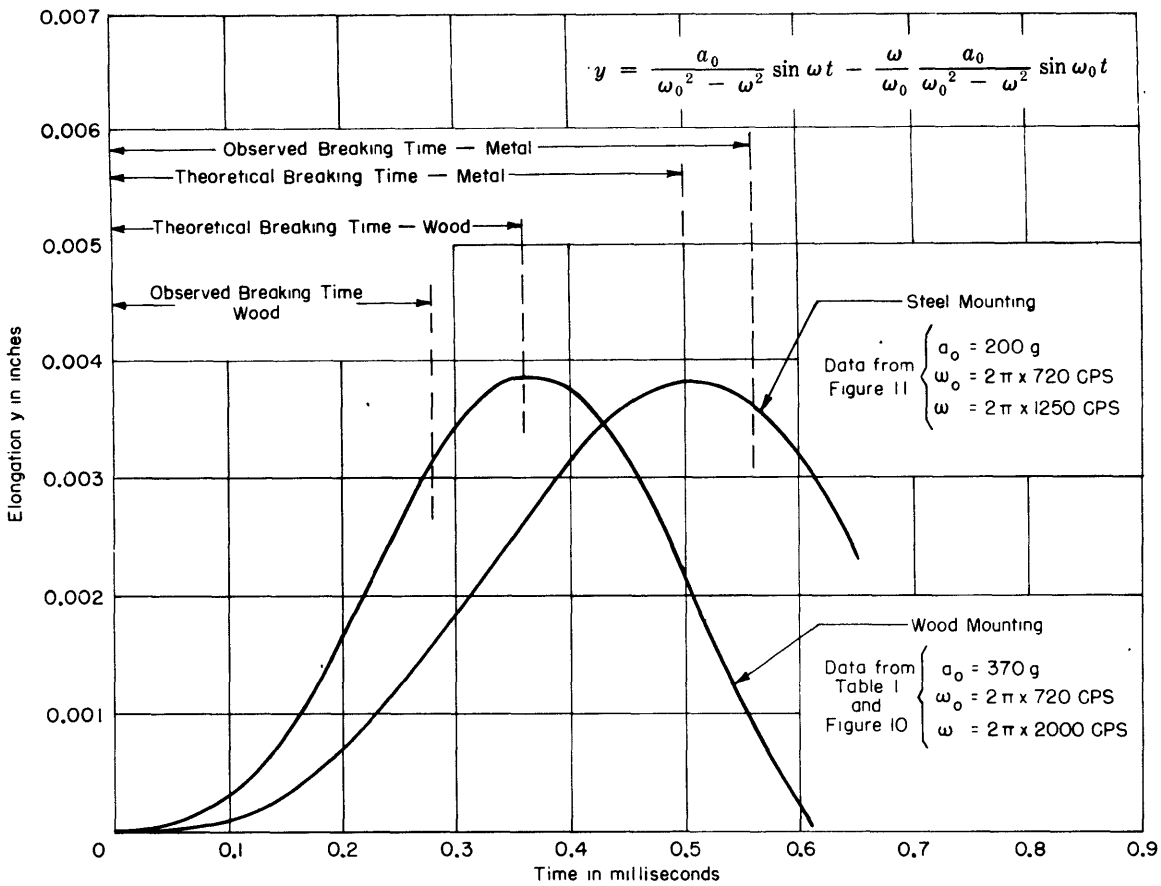

Figure 13 - Elongation of Neck Plotted against Time

The point of maximum elongation is the theoretical breaking point for the critical distance, and the time interval from zero to this maximum is the theoretical time required for fracture. Comparison of theoretical breaking times with the times obtained experimentally is shown on the curves in Figure 13. The agreement is not exact but is considered good in view of the assumption that the initial cycle is a sine wave.

Another check is made by obtaining the value of maximum elongation from the curves of Figure 13 and multiplying this value by the spring constant of the plugs in pounds per inch. The result is the force which caused rupture, since it has been assumed that the point of maximum elongation is the breaking point at the critical distance. Division of this force by the effective mass gives an acceleration that should equal the design value of 200 g. The actual values computed in this way were 201 g for gages mounted on wood and 198 g for gages mounted on metal, indicating that the tension at failure under dynamic loading equals that found for static loading.

The elongation at failure, obtained from the static stress-strain curves, approximates the two maximum extensions in the theoretical curves of Figure 13. The elongations obtained statically range from 0.0025 to 0.004 inch.

FURTHER DEVELOPMENT OF FIRST-CYCLE-BREAKAGE THEORY

It appears from the preceding discussion that the mass-plug accelerometer under dynamic loading failed at the same tension and elongation of the neck which produced failure under static loading. The peak accelerations at failure, however, may vary widely. This point is borne out by the experimental data and may be demonstrated theoretically by some additional manipulations of Equation [8]. The results obtained will apply not only to mass-plug accelerometers but also to other systems of a single degree of freedom.

Differentiating Equation [8] gives the velocity

$$\frac{dy}{dt} = \frac{a_0 \omega \cos \omega t}{\omega_0^2 - \omega^2} - \frac{a_0 \omega \cos \omega_0 t}{\omega_0^2 - \omega^2} \qquad [9]$$

At maximum displacement the velocity is zero and Equation [9] reduces to

$$\cos \omega t = \cos \omega_0 t$$

One solution of this equation is $t = t_0 = \frac{2\pi}{\omega + \omega_0}$, where t_0 is the time to the first maximum displacement.

Substitution of $\frac{2\pi}{\omega + \omega_0}$ for t in Equation [8] yields the following expression for the first maximum displacement:

$$y_{max} = \frac{a_0}{\omega_0^2 - \omega^2} \sin\left(\omega \frac{2\pi}{\omega + \omega_0}\right) - \frac{\omega}{\omega_0} \frac{a_0}{\omega_0^2 - \omega^2} \sin\left(\omega_0 \frac{2\pi}{\omega + \omega_0}\right) \qquad [10]$$

Multiplying both sides of Equation [10] by ω_0^2, replacing $y_{max}\, \omega_0^2$ by a, the statically determined breaking acceleration, and dividing by a_0 yields

$$\frac{a}{a_0} = \frac{\omega_0^2}{\omega_0^2 - \omega^2} \sin\left(\omega \frac{2\pi}{\omega + \omega_0}\right) - \omega_0^2 \frac{\omega}{\omega_0} \frac{1}{\omega_0^2 - \omega^2} \sin\left(\omega_0 \frac{2\pi}{\omega + \omega_0}\right) \qquad [11]$$

For ease of handling set $\frac{\omega_0}{\omega} = q$ and invert Equation [11], which gives

$$\frac{a_0}{a} = \frac{q^2 - 1}{q} \div \left[q \sin \frac{2\pi}{1 + q} - \sin \frac{2\pi q}{1 + q}\right] \qquad [12]$$

Equation [12] can be written in the simpler form

$$\frac{a_0}{a} = \frac{q - 1}{q \sin \frac{2\pi}{1 + q}} \qquad [13]$$

by noting that

$$\sin\frac{2\pi q}{1+q} = \sin\frac{2\pi(q+1-1)}{1+q} = \sin 2\pi\left(1-\frac{1}{q+1}\right)$$

$$= \sin\left(2\pi - \frac{2\pi}{1+q}\right) = -\sin\frac{2\pi}{1+q}$$

and hence

$$\frac{a_0}{a} = \frac{q^2-1}{q} \div \left[q\sin\frac{2\pi}{1+q} - \sin\frac{2\pi q}{1+q}\right]$$

$$= \frac{q^2-1}{q} \div (q+1)\sin\frac{2\pi}{1+q} = \frac{q-1}{q\sin\frac{2\pi}{1+q}}$$

The ratio a_0/a is plotted against ω_0/ω in Figure 14 for the range of $\omega_0/\omega = 0.1$ to $\omega_0/\omega = 10$.

It will be noted that the ratio of peak acceleration at failure to the design acceleration varies widely, depending on the ratio of resonant frequency to applied frequency. As the applied frequency is made smaller, ω_0/ω and a_0/a become indefinitely large, a_0/a approaching $\omega_0/2\pi\omega$. For small values of ω_0/ω, a_0/a approaches $\omega^2/2\pi\omega_0^2$. If any three of the quantities a, a_0, ω, and ω_0 are known, the curve can be used to determine what the fourth will be at the critical point

DELAYED BREAKAGE DUE TO RESONANCE

Figure 7 on page 10 is an example of the effect of resonance between a mass-plug accelerometer and its support. It will be noted that the displacement built up progressively and that failure occurred during the fifth cycle.

After it had been silvered, the plug which gave this record was polished with a cloth. This greatly increased its electrical resistance and essentially converted it into a strain gage. Apparently this plug had a slightly longer neck* than most of the other plugs, which made its natural frequency lower. Apparently the unit of which this plug was a part had a natural frequency very close to the driving frequency which is shown on the acceleration curve in Figure 10, peaks A, B, C, and D. After 4 cycles the plug acquired sufficient displacement to break. Breakages of this type show

* The neck length should be a constant for all plugs, but owing to their configuration and the material of which they are made, the tolerance cannot be kept within the closest limits desirable.

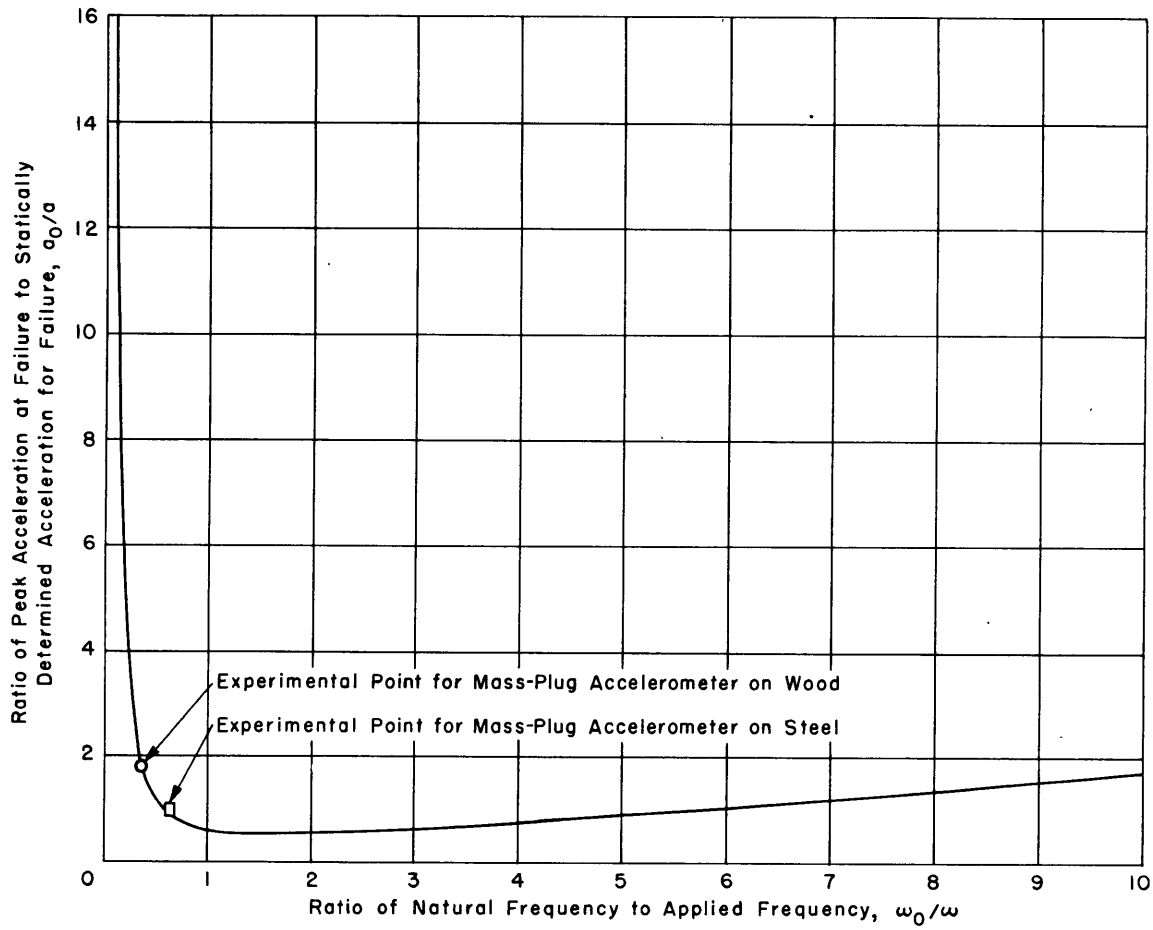

Figure 14 - Relation between a_0/a and ω_0/ω

This curve applies only when breakage occurs during the first cycle and when the driving motion is sinusoidal.

that it is possible for the driving impulses successively to decrease in amplitude but still drive the plug so that resonance is built up. The only requirement for this set of conditions would be that a driving pulse, though less than the one which preceded it, would still be of sufficient magnitude to overcome the damping in the mass-plug system. Figure 7 on page 10 is the clearest example of resonance rupture, but other records tend to substantiate the theory. Figure 8 on page 10 illustrates rupture on the second cycle. The oscillations are not as clearly defined, but this plug was not polished, did not act as a resistance strain gage, and showed only a slight disturbance on the record prior to breaking.

The plug whose motion is recorded in Figure 9 did not break, but oscillations appear on the trace which indicate that the plug was vibrating. The coating of silver was too thick to give a strain record, but there is

sufficient evidence to show that the plug was undergoing stress cycles. The frequency indicated on the record, however, was 710 cycles per second which was too high for resonance at the driving frequency which was acting when the record of Figure 10 was obtained. Since the indicated frequency is close to 720 cycles per second, it seems that the plug should have broken during the first cycle like most of the others. The natural frequency, however, is just one of the conditions which determines breakage at the critical distance and if any of the other determining conditions changed appreciably, rupture would not occur. The most likely source of variation in these experiments would be the peak acceleration, which, in turn, is dependent on the magnitude of the explosion. If a charge were slightly undersized, the peak acceleration would be reduced; this acceleration is one of the determining conditions for rupture. This may have happened in the present instance. It is also possible, however, that the neck of the plug was thicker as well as longer than that of the other plugs, so that its natural frequency was the same as that of most of the others, but its breaking strength was greater. This would change the acceleration necessary for failure, which is another one of the determining conditions.

CONCLUSIONS

The foregoing discussion leads to the following conclusions on the mass-plug accelerometer as a peak-reading instrument:

1. If the frequency and rated acceleration of the plug are known, then, in order to obtain accurately the magnitude of the driving acceleration, it is necessary to know also when the plug breaks and the shape of the driving motion.

If the driving motion is assumed to be sinusoidal, or of some other standard form, then it is necessary to know the frequency of the input motion as well as the time of breakage.

2. If it is known that the plugs broke on the first peak, then Figure 14 indicates that over a wide frequency range the plugs can be used to give a rough indication of the actual peak acceleration even if the driving frequency is unknown. Note also that the actual peak acceleration is always greater than approximately 55 per cent of the rated acceleration, again under the assumption of first-cycle breakage.

3. If it is not known that the plug broke on the first cycle, analysis of the breakage is impossible without a complete time-acceleration curve of the driving motion and a complete relative time-displacement curve of the plug.

REFERENCES

(1) TMB CONFIDENTIAL Report R-156, July 1943.

(2) TMB CONFIDENTIAL Report R-185, November 1943.

(3) "A Vibration Manual for Engineers," by R.T. McGoldrick, TMB Report R-189, March 1944.

(4) "A Method of Estimating Equivalent Statis Loads in Simple Elastic Structures," by G.E. Hudson, Ph.D., TMB Report 507, June 1943.